



HHS Public Access

Author manuscript

Wiley Interdiscip Rev Nanomed Nanobiotechnol. Author manuscript; available in PMC
2017 May 01.

Published in final edited form as:

Wiley Interdiscip Rev Nanomed Nanobiotechnol. 2016 May ; 8(3): 334–354. doi:10.1002/wnan.1365.

What is the role of curvature on the properties of nanomaterials for biomedical applications?

Estefania Gonzalez Solveyra and

Department of Biomedical Engineering, Department of Chemistry and Chemistry of Life Processes Institute, Northwestern University

Igal Szleifer

Department of Biomedical Engineering, Department of Chemistry and Chemistry of Life Processes Institute, Northwestern University

Igal Szleifer: igalsz@northwestern.edu

Abstract

The use of nanomaterials for drug delivery and theranostics applications is a promising paradigm in nanomedicine, as it brings together the best features of nanotechnology, molecular biology and medicine. To fully exploit the synergistic potential of such interdisciplinary strategy, a comprehensive description of the interactions at the interface between nanomaterials and biological systems is not only crucial, but also mandatory. Routine strategies to engineer nanomaterial-based drugs comprise modifying their surface with biocompatible and targeting ligands, in many cases resorting to modular approaches that assume additive behavior. However, emergent behavior can be observed when combining confinement and curvature. The final properties of functionalized nanomaterials become dependent not only on the properties of their constituents but also on the geometry of the nano-bio interface, and on the local molecular environment. Modularity no longer holds, and the coupling between interactions, chemical equilibrium and molecular organization has to be directly addressed in order to design smart nanomaterials with controlled spatial functionalization envisioning optimized biomedical applications. Nanoparticle's curvature becomes an integral part of the design strategy, enabling to control and engineer the chemical and surface properties with molecular precision. Understanding how NP size, morphology, and surface chemistry are interrelated will put us one step closer to engineering nanobiomaterials capable of mimicking biological structures and their behaviors, paving the way into applications and the possibility to elucidate the use of curvature by biological systems.

Introduction

The immense progress achieved during the past few decades in manipulating materials down to the nanoscale¹ has catapulted nanotechnology and nanomaterials into a myriad of different applications, ranging from electronics and technology,^{2, 3} development of new

Correspondence to: Igal Szleifer, igalsz@northwestern.edu.

Author declares no conflicts of interest.

sources of energy and environmental remediation,^{4–6} to biomedical therapeutics and diagnosis.⁷ Among the later, nanomaterials-based theranostic has emerged as a very promising paradigm, taking advantage of nanotechnology, molecular biology, and medicine, to engineer multifunctional nano-constructs that combine inorganic moieties, soft matter and biological entities for the dual purpose of improved therapy and diagnosis.^{8,9} Developing these nano-systems is a challenging task, as it combines properties of very different kinds of materials. Active work is done towards developing nanomaterials not only as drug delivery carriers, but as *smart* nanoplatforms, environmentally responsive, with maximized biospecificity.^{10,11} Orchestrating a specific *in vivo* effect by such nanocomposites and fine-tuning their responsiveness requires however a fundamental understanding of the interactions between them and the biological matrix.¹² This step is crucial to fully exploit the synergistic potential of this interdisciplinary approach, and translate it into a rational design of integrated nano-systems that can diagnose, deliver targeted therapy and monitor the response to therapy,¹³ ultimately making theranostics and personalized nanomedicine a near future possibility.⁹

Great advances have been done in developing sophisticated therapeutic agents,^{7,14} but still the keys to a rational design remain elusive. The reason lies in the complexity of the faced problem: biological matrices are multicomponent systems in which the effective interactions acting at cellular and sub-cellular levels are far from being of additive nature.^{15–18} The total is not simply the sum of the parts, and this translates into a coupling between molecular organization, physical interactions and changes in chemical state that has to be expressly addressed in order to attain a comprehensive picture of the different processes taking place.¹⁹ Interfacing nanomaterials with biological systems adds new levels of complexity and non-additive behavior, making difficult for existing experimental techniques and molecular models to obtain an accurate description of the system. The lack of such knowledge maybe one of the main reasons why nanomaterials translating into clinical applications has still not reached its full potential.^{14,20}

Literature covering nanomaterials as nanoplatforms for theranostic applications is abundant,^{21–23} yet there are scarce examples that attempt to present a comprehensive description on how the design parameters affect the responsiveness and behavior of the final construct. Experimental techniques are far from solving this problem on their own, but combining experimental efforts with the molecular detail provided by adequate modeling and theoretical frameworks may hold the key to fully describe the nano-bio interface and clarify the roles of the system's parameters, mainly the nanomaterial curvature, in its final properties. This goal is the central aim of this review, stressing the importance and potential of hybrid strategies that combine molecular modeling with state of the art experimental techniques to complete the description of complex biochemical life processes.

The literature revised in this review refers mainly (although not exclusively) to the use of nanoparticles (NPs) in cancer therapy. The discussion, however, will be oriented towards curvature effects at the nano-bio interface from a physicochemical perspective, and it is relevant to other nanocomposites facing different pathological conditions. To that end, we will describe succinctly the current scenario of nanomaterials envisioned for biomedical applications. Then, we will discuss in detail selected experimental and molecular modeling

studies that illustrate the role played by curvature in very relevant biomedical scenarios: NP charge regulation (pH responsive nanomaterials), protein adsorption on NP, interactions with membranes and cells, and NP-based biosensing.

Designing smart nanomaterials for biomedical applications

Biological systems consist in complex mixtures of diverse biomolecules, with hierarchical energy and length scales that orchestrate different processes. Directionality and anisotropy are constants in life design, allowing for a very precise control of the interactions and the overall fate of living organisms, from the molecular nature and spatially controlled architecture of cells to higher levels of organization (tissues, organs, specimens, populations). Controlling the spatial decoration of 3D nanomaterials is key to exert specific effects at the biomolecular level.

Nanomaterials with length scales of a few tens of nanometers constitute ideal platforms to link the physicochemical behavior at the nanoscale with the sophistication of biological systems.²⁴ Their fate in biological environments lays between the surface of the engineered nanomaterial and the surface of the multiple biological components (proteins, cell membranes, nucleic acids, antibodies, etc.) it encounters.²⁵ Interactions at the interface comprise a competition between chemical (acid-base and redox equilibrium, ligands-receptor binding) and physical interactions (Van der Waals, electrostatic interactions, hydrogen bonds) acting on different length and energy scales,¹⁹ and the result depends on a global balance, difficult to elucidate *a priori*. Surface modification of NPs has all the elements to modulate the interactions at this interface: the great advances achieved in synthetic and materials chemistry allows tuning the NP surface functionalization,²⁶ and ultimately manipulating the nano-bio interface.

A comprehensive design of nano-constructs for drug delivery and imaging applications implies selecting the most suited nanoplatform and determining its optimal parameters, establishing the route of administration, and optimizing the drug delivery performance by engineering its surface. Particular requirements must be met in order to successfully direct a desired effect to specific subsets of cells, with low (or non) toxicity for healthy tissue.²⁷ Foremost, such nanoconstructs should be water-soluble (i.e. hydrophilic) and exhibit a biodistribution as specific as possible. *In vivo* applications also imply that they must be able to surmount the biological barriers that exist from the administration point to their final destination: avoid capture by reticuloendothelial system and clearance by innate immunosystem, reach the targeted subset of cells, and exert their therapeutic effect.^{7, 28} The cycle is completed taking into account the final nano-systems' biocompatibility, biodegradability, and toxicity.^{29, 30}

Given the nanosized dimensions of the system, every physicochemical property has great impact in its final behavior and could be tuned as to engineer a specific performance *in vivo*: from the chemical composition of the nanomaterial, its size and shape, surface coating, surface charge, its hydrophobicity, to its surface roughness and rigidity.¹² Chemical modification of the NPs surface is key to for immunomodulation and biocompatibility, enhanced biodistribution, and site-specific recognition.³¹ Meanwhile, the size and shape of

the NPs also play a crucial role in the transport, delivery and cellular uptake mechanisms.^{7, 32} Figure 1 collects the design parameters in hand when engineering smart nanomaterials for optimized biomedical performance.

Nanoplatforms for theranostic applications

The collection of nanomaterials suited for the task is vast and expanding promptly: quantum dots,³³ metallic nanoparticles (iron³⁴ and gold³⁵ mainly), upconversion nanoparticles,³⁶ silica nanoparticles,³⁷ carbon nanotubes (CNTs),²⁸ polymer-based carriers (polymeric nanoparticles,¹² micelles,³⁸ dendrimers³⁹, and nanogels⁴⁰), lipid based-vehicles (liposomes),⁴¹ and viral NPs and bacteriophages.⁴² A survey of biomedical literature shows that the use of the term “nanoparticle” actually extends beyond its strict definition, and is used to encompass nanomaterials of different nature. This will also be the criterion used henceforth.

The progress achieved in recent years in the synthesis of NPs allows tailoring their sizes and shapes with remarkable control, ranging from a few to hundreds of nanometers, and spherical or non-spherical morphologies (rods, cages, disks, stars, nanoshells) at command.^{43, 44} Spherical NPs have been more exploited in biomedical research so far (given their easier preparation), but important efforts are also directed towards the development of anisotropic NPs with edges and spikes, as they hold promise in biosensing and in manipulating NP-cell interactions.^{45–47} In what follows, we will address the coupling of the nanoconstruct properties and its behavior in relevant biological processes, referring mainly to spherical NPs. However, our general conclusions on the complex coupling of interactions and the role of curvature are extensible to other morphologies. In addition, we will focus on surface functionalized NPs, where the atomic details of the bare NP surface are masked by the ligands grafted to them. The effects of the NP's surface atomic structure in biomedical scenarios are beyond the scope of the present review.

Drug delivery strategies

The first nanomedicines comprised mainly controlled-release polymeric NPs that improved drug circulation time and administration due to their pharmacokinetics and biodistribution.⁷ Since then, efforts have been directed towards delivering active agents more selectively to pathological sites by passive or active strategies, and, moreover, towards engineering environmentally responsive NPs that allow drug release at the target site in a temporal and spatial resolved manner.

Targeting strategies can be classified into passive and active. Passive targeting relies on the NPs intrinsic properties (shape and size) to achieve local accumulation, without resorting to affinity ligands. This non-selective strategy has been greatly exploited in cancer therapies, as solid tumors facilitate the accumulation of NPs due to their leaky and underdeveloped vasculature and lymphatic function. This effect is known as the “enhanced permeation and retention effect” (EPR), and since it's first documentation by Maeda and coworkers,⁴⁸ it has been widely described and used in different oncology applications.⁴⁹ Active targeting, on the other hand, resorts to ligand-mediated interactions in order to impart site-specific delivery, and consists in modifying the NPs surface with biological ligands known to bind to receptors

(over)expressed in specific cellular populations. This strategy, although more selective, requires a high level of differentiation between pathologic and healthy cells, in order to avoid toxic off-target effects.⁵⁰ Carefully selecting the targeting strategy allows to span selective tissue, cellular and organelle-specific targeting.^{7, 51} Commonly employed ligands include antibodies or fragments of them (nanobodies), proteins, peptides, nucleic acids (DNAs, micro RNAs, aptamers) and small molecules (carbohydrates or folic acid).^{52, 53}

Going further, a step forward would be to engineer bionanomaterials that can react to the different environmental conditions encountered from their initial administration point to their target site. Responsiveness is the foundation in the physical chemistry of life processes, and it is the ultimate tool to attain optimized drug delivery and specific biodistribution. It can also impart versatility to the systems, making them very suited as multifunctional platforms for targeted therapeutics and diagnosis. This can be achieved by coating the NP with responsive polymers or biological moieties.⁵⁴ The stimuli-responsive behavior derives from changes in the nanosystems' physicochemical properties,¹⁰ through an overall free energy balance that optimizes chemical equilibrium and physical interactions jointly. Stimuli can either be endogenous (pH,¹¹ redox potential,⁵⁵ differential enzyme concentrations⁵⁶) or exogenous (temperature,^{57, 58} magnetic field,⁵⁹ ultrasound,⁶⁰ light^{21, 61}). The selection of a given stimulus and responsive material provides for a wide range of mechanisms and schemes to choose from in order to engineer smart materials for a specific biomedical application.^{10, 62}

Why curvature matters?

Optimizing drug delivery strategies requires understanding the role of each design parameter graphically summarized in Figure 1 and, moreover, realizing that their impact on the final properties and behavior of the system is not independent from the others. In particular, NPs' curvature, through its size and shape, modulates the forces and molecular interactions,¹⁹ and hence should not be seen as an additive factor, but as a fundamental variable. Moreover, combining confinement and curvature gives rise to non-trivial effects, as the physicochemical and biomolecular properties of a compound immobilized onto nanosized NPs depend not only on its intrinsic properties but also on its local environment.^{19, 63}

NP's curvature plays a central role in its surface modification and the functionality of the final nanocomposite (attain colloidal stability and biocompatibility, target specific cellular types and subcellular organelles, and deliver agents on site), as it determines the available volume to the molecules grafted to its surface. Furthermore, the geometry of the NP defines whether this amount increases (curved convex NPs, spheres and cylinders for example), decreases (curved concave objects, like nanotubes), or remains constant (planar surfaces) as a function of the distance from the surface. Immobilizing a molecule onto a surface reduces its translational and conformational entropy with respect to the free molecule in solution in a way that greatly depends on the geometric constraint imposed by the surface. The penalty this imposes ultimately determines the molecular organization of surface species as well as their chemical state (protonated-unprotonated, bound-unbound, reduced-oxidized), as we will discuss in the following examples.

Charge regulation: pH responsive systems

Acid-base equilibrium provides a way to modulate the degree of protonation, and hence charge, of NP's surface groups, allowing to tune their interaction with biomolecules and biological entities through electrostatic forces. Many pH-directed drug delivery systems have been devised to take advantage of the pH differences encountered in organs, tissues and subcellular compartments, both in healthy and pathological conditions.¹¹ Oral delivery drugs use the pH gradients in the gastrointestinal tract. Targeting strategies to solids tumors have exploited the more acidic environment of the tumor (pH of 6–7) as compared to healthy tissues (~7.4). At a much smaller length scale, endosomal and liposomal acidification have also been used to direct and facilitate intracellular drug delivery.¹⁰

Mechanisms of pH-responsive NPs encompass pH-dependent swelling and dissolution, aggregation, drug dissociation and release, pH-labile linkers, pH-sensitive drug-polymers conjugates¹¹. The basic idea is to take advantage of the acid-base properties of the coating ligands and the way these properties change when the ligands are immobilized onto surfaces of different curvature and subject to different environmental conditions. In spite of the numerous and diverse NP-based constructs that exploit the response to pH changes, little is known about how the curvature affects the physicochemical properties and the responsiveness of the ligands.

Nap and co-workers conducted a thorough theoretical study on the effect of surface geometry and solution conditions (pH and ionic strength) on the acid-base equilibrium of weak polyelectrolytes tethered to planar, cylindrical and spherical surfaces (upper panels of Figure 2).⁶⁴ They found that the surface geometry plays a dramatic role in acid-base equilibrium as well as in the molecular organization of the coating layer. Figure 2 shows the variation of the local pH, defined as $\text{pH}(r) = -\log[\text{H}^+(r)]$, and the local degree of deprotonation (dissociation), $f(r)$, as a function of the distance from the surface for a variety of solution's ionic strength. Interestingly, they find that the degree of dissociation and the local pH change significantly with the curvature of the surface, for a given surface coverage of polymer and solution ionic strength. Moreover, the local variations within a few nanometers can be extremely large. Let us consider in detail their predictions for physiological ionic strengths, i.e. salt concentration of 0.1M (red curves in Figure 2). For a planar brush the degree of dissociation f within the film is 0.2, while in the bulk it is 0.5. This corresponds to local pH that can be around 6.4 in the film, compared to 7 in the bulk. For a spherical nanoparticle, the degree of dissociation of the polymeric acid groups close to the surface is 20% lower than in the bulk solution. The cylindrical particle shows an intermediate behavior between that of the two other geometries.

The question is what is the driving force for this behavior. The first thing to consider is that the volume available as a function of the distance from the grafting surfaces is constant for planar surfaces and it increases in a linear (quadratic) manner for cylinders (spheres). Therefore, for the same surface density, charging of end-grafted polymers leads to stronger electrostatic repulsions in the planar layer as compared to the sphere. The optimal response of the system is to shift the acid-base equilibrium to the uncharged species in order to reduce the electrostatic repulsions. This effect is more pronounced as the electrostatic repulsions increase, namely the effect is stronger for lower salt concentrations (green and blue curves).

The volume available for the different geometries explains the differences presented in Figure 2.

The dramatic changes in local pH and protonation state observed as a function of ionic strength, demonstrates the dual role that the solution salt concentration plays in pH-responsive systems. Namely, as the concentration of salt increases the screening length decreases and the electrostatic interactions become weaker. However, at the same time the systems acquire more charge making the electrostatic contribution more important. The interplay between molecular organization, physical interactions and chemical state is the basis for the emergent behavior observed as a function of pH and ionic strength.⁶⁴

Wang, Nap and co-workers combined titration experiments with a molecular theory to investigate the acid-base equilibrium of the terminal carboxylic group in Au-NPs of different sizes coated with self-assembled monolayers of mercaptoundecanoic acid (MUA) (scheme in the left panel of Figure 3).⁶⁵ Figure 3a shows the fraction (f) of charged/dissociated MUA on the NPs as obtained from experiments, and from calculations with their molecular theory and the Henderson-Hasselbach equation. It is evident from the results that the assumption of ideal solution behavior for the MUA tethered to the NPs is far from accurate, and so is the commonly applied Henderson-Hasselbach treatment. To characterize the dissociation of the acid groups, the authors obtained experimental values and molecular theory predictions of the apparent pK_a . This quantity is defined as the pH for which the degree of dissociation is 0.5. They found that its value is significantly higher than the pK_a of MUA in solution (~4.8) and that it strongly depends on the NP's diameter and the ionic strength of the solution (Figure 3b). This is again a manifestation of the dual role of the solutions ionic strength as well as the molecular organization of the ligands. Namely, the distance between acid groups depends on the NP size, the average distance between headgroups of MUAs decreases with NPs' increasing diameter, assuming the same surface coverage of ligands. Therefore, as the size of the NP increases it is harder to ionize the carboxylic head-groups. The results presented in Figure 3 emphasize the importance of considering the curvature environment on the design of NP coatings. Actually, a NP of size 7.2nm at physiological ionic strength will have marginal (or no) solubility at pH 7, very different from what would be expected from the solution pK_a of the MUA.

Similar arguments hold to rationalize the effect of NP curvature on the interfacial chemistry of metal oxide NPs in aqueous solutions, where the protonation/deprotonation of the surface metallic atoms defines the NP surface charge. Vayssieres studied the surface chemistry of maghemite ($\gamma\text{-Fe}_2\text{O}_3$) NPs, and found that the point-of-zero-charge (PZC) increases when the particle size decreases, with a variation of two units of pH between NPs of 12.0 and 3.5 nm, reflecting an increase in surface ionization with decreasing particle size.⁶⁶ A similar shift in the acid-base equilibrium to the right has also been reported for silica NPs.⁶⁷

Understanding charge regulation is of primary importance when engineering pH-responsive NP-based constructs, particularly when envisioning interactions with surfaces, as it constitutes a first step towards rationalizing their interaction with cells' membranes. Nap and co-workers studied the adsorption of acid and polymer coated NP onto positively and negatively charged planar surfaces.⁶⁸ They found the adsorption process is governed by the

charge of the adsorbing surface and the amount of deprotonated acid groups on the NP. As the NP approaches the charged surface, driven by van der Waals attractions, its weak acid groups regulate their charge in order to minimize electrostatic repulsions or maximize attractions (depending on the sign of the adsorbing surface's charge), resulting in an asymmetric charge distribution on the NP due to the symmetry rupture imposed by the surface. The global interplay between NPs' asymmetric charge and the charge of the adsorbing surface, modulated by the underlying curvature of the surface, determines the amount of adsorbing NPs. These results emphasize the importance of explicitly considering charge regulation (acid-base equilibrium) as a key mechanism for the responsiveness of the NPs to local changes in electrostatic potential and/or pH. We review below the dramatic effect that arises from combining pH and ligand-receptor binding with coated NP's interacting with lipid layers.

Viruses and virus-based nanocarriers are another example of the importance of charge regulation in biomedical applications. Virus particles consist of protein molecules that self-assemble into a hollow scaffold (capsid) enclosing the viral nucleic acid, and that spontaneously disassemble upon cue inside the host.⁶⁹ The underlying mechanism of the viral RNA or DNA packaging can also be used to pack other type of functional molecules, based on supramolecular self-assembly and disassembly processes. This process offers a way to engineer versatile constructs that can be easily functionalized for improved drug delivery. Through adequate protein design and genetic engineering, viral capsids can be used to encapsulate nucleic acids, enzymes, or charged (positively or negatively) molecules.⁷⁰ One way viruses protect their genetic material, survive the different environments of their hosts, and disassemble at the target site is by regulating the surface charge of the capsid. This, again, is accomplished by adjusting the acid-base equilibrium of the amino acids (i.e., their charge) in order to minimize the electrostatic repulsions between surface charges, salt ions and biological entities. The regulation of the charge state of the capsid is largely affected by the solution pH and salt ionic strength, which can induce a switch from net positive to net negative.⁷¹ This pH-responsiveness in viruses and virus-like NP is key to prepare stables carrier that would disassemble at the target site, specifically envisioning applications targeting the tumor acidic microenvironment or the acidic endosomal compartments of cells.

Protein adsorption & biofouling

NPs in biological environments interact with a diverse mixture of proteins, metabolites, peptides, and carbohydrates. Firstly, plasma or serum proteins adsorb onto the nanomaterial surface forming a 'protein corona'⁷² that imparts a *biological identity* to the NP,⁷³ determining its *in vivo* distribution, systemic clearance, downstream biological effects and reactivity in physiological media.⁷⁴ The formation of this protein corona is a multifactorial and dynamic process that depends on the NP properties (size, geometry, surface chemistry), the encountered proteins (identity and function), and the medium.^{75, 76} It is the NP-corona complex that interacts with the biological components, so controlling this process is of paramount importance for any given biomedical application.

It has been extensively established that nanomaterials with hydrophobic or charged surfaces tend to adsorb more proteins than neutral or hydrophilic surfaces.^{75, 77} The effect of the NP size has also been phenomenologically studied,^{75, 76, 78} although the interplay between curvature and surface chemistry in the final behavior of the system has been only scarcely addressed. Walkey and coworkers developed an extensive library of protein corona fingerprints for NP of different sizes and surface ligands (schemes in the panel A of Figure 4).⁷⁹ Resorting to a combinatorial and bioinformatics approach, they profiled the biological activities of 105 surface-modified Au-NPs, correlating the identities and abundance of the proteins in the corona with the cell association for each type of NP. As to protein adsorption, they found that NP of the same size modified with charged ligands (either cationic or anionic) enhanced protein-NP interactions, resulting in higher adsorption loads (Figure 4, panel B). On the other hand, NPs modified with neutral ligands were shown to better resist protein adsorption. Comparing NP with the same surface chemistry, smaller NPs tend to adsorb a higher density of proteins than larger NPs. This could be related with the available volume that proteins have when adsorbing onto NPs of different sizes, since the lower curvature, the lower the available volume at the same distance from the surface. This ultimately translates in stronger steric repulsions between adjacent adsorbed proteins and hence lower protein-adsorbed density. The extent of the effect depends on the nature of the coating (neutral, cationic, anionic). The authors' results reflect the non-trivial interplay between NP's curvature and surface chemistry on the protein-protein and protein-surface interactions. NP's curvature and surface properties have also been found to modify the composition of the protein corona developed around them.⁷⁵

The uncontrolled initial protein adsorption that bare nanomaterials are subject to in physiological media (also known as protein biofouling) limits their use as nanomedicines. Common strategies to prevent or control it consist on "passivating" the NP surface,⁷³ that is, grafting antifouling ligands onto it. Most widely used ligands include poly(ethylene glycol) (PEG),⁸⁰ but also other organic thin films, like self-assembled monolayers (SAMs),⁸¹ zwitterionic polymers,⁸² polysaccharides,⁸³ or peptoids.^{84–86} The layer of tethered molecules serves as a thermodynamic and/or kinetic barrier for the adsorption,^{87, 88} presenting a steric barrier to the proteins and giving rise to a repulsion that competes against the bare protein-surface attraction.⁸⁹ The antifouling efficiency depends on the molecular weight of the polymeric layer and the surface coverage,⁸⁹ but there is no clear understanding on the role played by the NP's curvature. Walkey and coworkers conducted a systematic experimental study of serum protein adsorption on Au-NP of different sizes, grafted with PEG molecules (Figure 5a).⁹⁰ The conformational freedom of the polymer chains depends on the NP curvature and the grafting density,⁹¹ and with that the entropic barrier they present to proteins. The available volume for the tethered molecules decreases with increasing NP size and also with increasing grafting density, since this implies higher compression between neighboring PEG molecules (Figure 5b). It is the interplay between NP size and PEG density that determines not only the total protein adsorption (Figure 5c), but also the composition of the protein corona (Figure 5d–g). It is important to mention that on curved surfaces not even the highest PEG surface density eliminates protein adsorption completely. This fact actually fuels the search for other biocompatible polymers with improved antifouling properties.^{84–86}

Gagner and coworkers studied the effect of Au-NP morphology (Au nanospheres, Au-NS, 10.6 nm diameter and Au nanorods, Au-NR, 10.3 nm diameter and 36.4 nm length) on the adsorption, structure and function of lysozyme (Lyz) and α -chymotrypsin (ChT).⁹² In order to obtain stable dispersions of the Au-NPs, their surfaces were modified with 16-mercaptohexadecanoic acid (MHDA). Protein adsorption experiments were carried out at pH=7.0, rendering electrostatics the primary interactions between the positively charged proteins ($pI_{Lyz}=11$ and $pI_{ChT}=8.75$) and the negatively charged MHDA-stabilized NPs ($pK_a\sim 4.8$). As can be seen in the adsorption isotherms in Figure 6a–b, the process is greatly affected by the NP morphology, although the extent of the effect is protein-specific. The authors found that the surface density of adsorbed proteins was higher on AuNR than AuNS, and suggested that a smaller curvature would facilitate protein-protein interactions and hence a higher packing density of proteins. Based on the similar diameters of the Au-NS and the Au-NR, the authors also hypothesized that the surface density for the spherical ends of the NRs is lower than for the cylindrical body of them, implying an anisotropic distribution of proteins driven by curvature differences. This reflects the impact of curvature on both protein-surface and lateral protein-protein interactions, along with possible charge regulation effects, signature of non-trivial coupling between the physical and chemical interactions acting in the system. Important differences were observed between the two proteins of the study, highlighting the role of protein identity in this process. In the case of lysozyme, adsorption on both AuNS and AuNR lead to aggregation and reduced enzymatic activity. Inspection with circular dichroism spectroscopy revealed changes in the protein conformation, which were proposed to account for Lyz-Au NP conjugates aggregation and activity loss. On the other hand, no aggregation was observed for the α -chymotrypsin on either AuNS or AuNR, and multilayer protein adsorption was reported for the ChT-AuNR conjugate (Figure 6c). Conformational analysis at different surface coverages evidenced no significant changes upon adsorption in sub-monolayer conditions, an important loss in secondary structure when reaching monolayer coverage, and no greater effects in subsequent layers. The authors rationalize their findings by separating the adsorption process of both proteins into three regions: an initial binding that occurs with almost no conformational change of the adsorbed proteins molecules, a transition stage characterized by a combination of protein-surface and protein-protein interactions that result in conformational changes, and a final stage of multilayer adsorption (Figure 6d). The results reported in this work highlight the importance of both NP morphology and curvature and protein identity on the adsorption process and the interactions of NPs in biological fluids. It can also be appreciated that a complementary theoretical study would greatly enrich the authors' findings, as it could provide molecular detail and direct evidence of facts that were inferred from the experimental data, thus providing a more complete description of the system.

Molecular modeling and theoretical approaches that describe the adsorption and binding processes of proteins onto planar surfaces are abundant, yet there are almost none for curved NPs. Multi-scale approaches, spanning from atomistic to coarse-graining simulations, have provided valuable molecular descriptions of surface-protein interactions, protein conformational changes upon adsorption, most probable structures for protein-NP complexes, or the role played by different protein residues during folding or unfolding processes.⁹³ Numerous studies on antifouling behavior of polymer-coated planar surfaces

have been done resorting to analytical theories⁹⁴ and the molecular theory developed in our group.^{85, 87, 95–97} However, the molecular significance of the NP's curvature on the process of protein adsorption and the antifouling performance of surface-modified NPs has not been thoroughly addressed. Experimental information is rather disperse and heterogeneous,⁷⁶⁷⁴ so a theoretical approach would contribute greatly to gain insights into a fundamental understanding of protein-nanomaterial interactions.

Interaction of NPs with membranes: Ligand-receptor binding and cell internalization

Successful drug delivery strategies encompass not only surviving clearance by the immune system and reaching the targeted site, but also releasing the therapeutic or diagnosis agent within the cell. There are mainly two mechanisms for crossing the cell membrane into the cytosol or into sub-cellular organelles: endocytosis and direct translocation.⁹⁸ The first of them involves the membrane engulfing molecules from the extracellular plasma and forming an endosome that is then released into the cytosol. This process is typically associated with the transport of large polar molecules that cannot simply pass through the hydrophobic core of the cell membrane. The endocytosis pathways can be further classified with respect to the different proteins and lipids involved in the process. But in general terms, it occurs via specific binding events between receptors at the membrane and targeting ligands used to functionalize the NP surface (receptor-mediated uptake), or by direct association with the membrane (non-receptor-mediated uptake), dictated by NP-membrane hydrophobic and electrostatic interactions.⁹⁸ Endocytosis also plays a significant role in surface receptor regulation (including antigen presentation) and in the control of several signaling cascades.⁹⁸ Translocation, on the other hand, allows for the direct passage of certain molecules into the cytosol, without the formation of vesicles. The advantage of avoiding endosomal encapsulation is that no further strategy is needed to escape from it once inside the cytosol.

In the last decades, an extensive amount of work and data on NP-membrane interactions and NP internalization pathways has been produced.⁹⁹ However, the factors that determine which path is followed and the mechanisms that regulate them are not yet clear.⁹⁸ Cell-NP interactions, uptake mechanisms and intracellular trafficking are governed by the physicochemical properties of the NP, mainly size, shape and surface properties (surface charge, hydrophobicity, targeting ligands),¹⁰⁰¹⁰¹ and also by the cell properties, such as cell type, cycle phase, and cell membrane properties (lipid packing, membrane curvature).⁹⁹ Moreover, the interaction with NPs triggers responses and changes in the membrane itself, making this a process difficult to rationalize and understand.¹⁰² Existing experimental techniques are challenged by the nanoscale nature of the process and the complexity of the nano-bio matrix, and in many cases are bound to infer molecular information from macroscopic results. Theoretical and modeling methods are well suited to provide insights that may help fill this gap. However, modeling the NP-cell membrane interactions is a very challenging task as well, due to the multi component nature of the systems and the wide range of relevant length and time scales to be considered. The combination of experimental observations and theoretical approaches holds great promise into solving the new paradigms in nanomedicine as they enable the link between molecular information and macroscopic observations.

NPs size and shape have a major effect on cell penetration, modulating the uptake efficiency and kinetics, the internalization mechanism, and their intracellular distribution (see also Figure 4C).^{46, 47, 103} In terms of NP surface charge and hydrophobicity, cationic NPs are in general more efficiently internalized, due to stronger interactions with the negatively charged groups on the cellular surface. However, efficient uptake of negatively charged NPs has been reported as well (see also Figure 4C).¹⁰⁴ The arrangement of the NP surface-ligands has also been proposed to affect the cell-NP interactions, and hence the mechanism of internalization,¹⁰⁵ although these findings have been the focus of some controversy in the research community.¹⁰⁶

Nap and coworkers conducted a theoretical study on the effect of confinement and surface rearrangement on the binding of a polymer micelles to a planar surface, process relevant not only to achieve targeted delivery and cellular uptake but also for cell signaling. The surface of spherical micelles was modified with a binary mixture of neutral polymers of different chain length, the shorter ones being end-functionalized with a ligand that binds to the surface receptor (scheme in Figure 7a).¹⁰⁷ The authors chose nanosized micelles over NPs since polymer molecules on the surface of the micelles are laterally mobile within the self-assembled structure, while they are laterally immobile when chemically grafted to NPs' surfaces. This allowed them to study the effect of ligand mobility in the final binding properties of the nanoconstruct. They predicted that as the micelle approaches the surface, the shorter chains preferentially locate themselves between the micelle and the surface, while longer chains diffuse and become more concentrated on the opposite side (Figure 7b). This anisotropic distribution of surface molecules reflects the interplay between the lateral mobility of ligands, the repulsions between tethered chains induced by confinement, and the binding events between micelle-ligands and surface-receptors. The micelle's curvature modulates the coupling between them. Moreover, the balance of these factors can enhance the interactions between the polymer-coated micelle and the surface, as reflected in the free energy changes upon binding for nanosystems functionalized with mobile vs. immobile polymers (Figure 7c), representing possible scenarios of binding of functionalized micelles or chemically modified NPs.

In a later publication, Nap and coworkers analyzed how lipid composition and charge regulation would affect the binding of nano micelles to membrane receptors.¹⁷ They studied the interactions between coated micelles with three different model membranes: (i) neutral lipid membrane with overexpressed receptors, (ii) membrane with negatively charged lipids and (iii) membranes with both overexpressed receptors and negatively charged lipids. Micelles were functionalized with a binary mixture of short neutral polymers and polybases (which can become positively charged, $pK_a=7.5$) with a functional end-group for specific binding to the membrane-receptors (scheme in Figure 8a). Results show that combining ligand-receptor binding events and electrostatic attractions leads to a very pronounced segregation between the neutral and charged polymers on the micelle surface (Figure 8b). This in turn is accompanied by a change in the charge state of the polybase molecules on the micelle and of the lipid molecules in the membrane (Figure 8c, left and right panel respectively). The solution's pH is equal to the bulk polybase pK_a , so a fraction of dissociated groups of $f=0.5$ would be expected. However, at almost all distances from the micelle surface the fraction of protonated groups is much smaller than that. (Figures 8c left

panel). This is due to the fact that the local density of basic groups in the micellar corona is large. Given this constraint, the system pays chemical free energy to minimize electrostatic repulsions by regulating the polybase charge towards the unprotonated state. This results in a much lower fraction of charged bases in the micellar corona compared to individual bases in bulk solution, with the only exception of two points in the region close to the lipid layer. In these regions, the fraction of charge is enhanced due to the attractions between the charged lipids and polybases and the release of confined counterions. The lowest values of protonation are obtained for the region between the nano micelle and the membrane surface, where the concentration of polybases is even higher (Figure 8b right panel). An analogous charged segregation is observed between the lipid molecules in the membrane (Figure 8 left panel). The results of this study reveal that local charge regulation, molecular reorganization and optimization of multiple interactions, modulated by the micelles curvature, excerpt non-additive effects and result in a much larger binding (blue line, Figure 8d) than the one corresponding to the sum of the independent contributions (red and purple lines, Figure 8d). Even more striking, there are regions of interaction between the micelle and the membrane where combining two effective repulsions leads to an overall attraction. It is important to mention the significant role of local pH when considering interaction with membranes lipids, as it provides a way to modify binding by several orders of magnitude. This can be achieved by modifying the proportion of charged lipids in the membrane.¹⁷ The authors' findings constitute a good example on how to improve targeting by using multiple physical and chemical interactions. This polyvalency strategy is already used in nature by many viruses and bacteria,¹⁰⁸ and it's becoming a powerful tool to design and engineer multivalent NPs with enhanced selectivity and binding.^{109, 110}

Alexander-Katz and coworkers have proposed different mechanisms of membrane translocation for neutral and anionic small NPs (diameter<10nm), and for cationic NPs to directly cross the lipidic membrane. In the case of neutral or anionic NPs, the insertion of the NP in the bilayer core was found as the crucial step towards reaching the cytosol.^{111, 112} Meanwhile, for cationic NPs the translocation mechanism seems to comprise the formation of transient holes on the membrane.¹¹³ Van Lehn and coworkers conducted experimental and theoretical studies of the uptake of Au-NPs functionalized with a mixture of 11-mercaptoundecane sulfonate (MUS) and octanethiol (OT) of different composition and surface morphology (Figure 9A–B).¹¹⁴ They found that there was a critical size below which the insertion in the bilayer is favorable, and that it depends on the composition of the NP-surface coating. Their calculations predicted that the functionalized NPs could embed into the membrane core for sizes below a certain value, that depends greatly on the surface composition, in very good agreement with experiments (Figure 9C–D). No significant effect of the NP-surface morphology was observed (Figure 9C). Based on their results, the authors rationalize that the insertion of the NP in the bilayer is driven by the hydrophobic interactions between the OT molecules and the bilayer core, while the charged head-groups of the MUS molecules “snorkel” towards the exterior of the membrane (see Figure 9A for a schematic representation). This phenomenon is directly related with the available volume for the hydrophilic ligand to explore: embedding depends on the ability of the NP surface monolayer to deform and match the lipid bilayer, and is thus governed by the NP curvature and the ligand flexibility.¹¹⁵ Regarding the role of particle morphology, Yang and coworkers

modeled the interactions of anisotropic NPs with membranes, finding that the geometrical properties of the NP (size and shape), and its orientation with respect to the bilayer greatly affects the internalization process.¹¹⁶ These findings imply that by controlling the orientation of anisotropic particles, it is possible to improve targeting and uptake of NPs to specific cells.

The examples discussed above reflect the huge effects of curvature and coupled interactions in systems below 10 nm in size. The use of nanomicelles in this size range for drug delivery presents the advantage of exploiting the curvature of the aggregate to tune the interactions with the cell membrane. However, they present limitations in the amount of drug that can be carried, and therefore larger concentrations of carriers may be needed. Tuning the balance between cargo amount and interactions is an important consideration in the design of nanocarriers and should be explicitly considered for each drug delivery application.

Sensing, imaging & biodiagnostics

Modulating the responsiveness of functionalized NPs by their interaction with target biomolecules opens the door to a myriad of applications in biosensing and biodiagnostics. Given their optical,¹¹⁷ magnetic¹¹⁸ and photoacoustic properties,^{119, 120} NPs are promising platforms in those areas as their intense response to incident radiation can be linked to the presence of a target molecules, offering extremely sensitive detection in solution. In general, NPs biosensors comprise a surface-grafted biomolecular recognition element that specifically interacts with the target analyte, and a transducer element that transform the analyte-receptor event into a particle-derived signal.¹²¹ Between the diverse biosensing mechanisms that exist, fluorescence and plasmon based mechanisms are the most common, each with specific surface-bound biomolecular constructs. In both cases, the analyte-receptor interactions activate the biosensing mechanisms that modulate the NP properties.¹²¹ Tuning the interface between the nanomaterial and its surroundings is crucial to maximize sensitivity and specificity.¹²² In what follows, we will focus our analysis on plasmonic nanomaterials and their relevance for biodiagnostics.

Metal nanoparticles exhibit a surface plasmon resonance (SPR) peak, which position can be related to the presence or the absence of target biomolecules. The optical excitation of surface plasmons in NPs confines the electromagnetic fields, giving rise to a localized surface plasmon resonance (LSPR) that in plasmonic NPs translates into an intense peak in the visible range, and into strong electromagnetic fields at the particle surface. Resonance conditions (i.e. incident light with the same frequency of the NP's LSPR) depend on the NP surface ligands, and their interactions with molecules in solution. The position of the LSPR peak changes with NP's shape, size, surface functionalization, and aggregation behavior, and is modulated by the interactions with target analytes.^{117, 121, 123} Tuning the LSPR absorption band by carefully engineering the NP construct is key for biomedical applications, as a shift to NIR range of the electromagnetic spectrum is ideally suited for *in vivo* applications,¹²⁴ such as photothermal treatments, photodynamic therapy, IR fluorescence imaging, or surface-enhanced Raman scattering imaging and sensing.⁶¹ However, optimal NP engineering is not trivial and requires consideration of all the design parameters jointly. An example of such not trivial behavior are the results of a recent

experimental and theoretical study by Peng and coworkers, in which they reported a non-monotonic dependence of the Ag-NP SPR adsorption band with decreasing NP size, observing an initial blue-shift followed by a strong red-shift.¹²⁵ Based on their theoretical modeling, the authors associated this behavior with a lower conductivity in the outer metallic layer due to the interactions with the surface ligands. This hypothesis was experimentally confirmed by ligand exchange titrations, reaffirming the effect of the NP's coating on the SPR peak position.¹²⁵ Tagliazucchi and coworkers carried a study on the plasmonic properties of Au-NPs coated with polymers responsive to changes in the temperature (solvent quality).¹²⁶ Resorting to a combination of molecular theory and electrodynamic calculations, the authors were able to analyze structural, thermodynamic and optical properties of the system, concentrating on the shift of the LSPR absorption band upon polymer collapse driven by changes in the solvent quality (scheme in Figure 10 a). Results showed a red shift in the LSPR peak upon polymer collapse, which magnitude depends in a non-monotonic way on the NP radius (scheme in Figure 10 b–c). They also discussed that the size and shape effects on the polymeric layer structure would have direct impact on the plasmonic coupling between NP, as they modulate the distance between them. These results suggest that engineered nanoparticles used for biosensing may change their reporting behavior due to changes in the environment, and this fact should be considered in the designing stages of the material. Understanding the effects of shape, size, surface functionalization, and aggregation behavior on the optical properties of smart NP constructs is crucial for a rational design of nanomaterial-based biosensors.

Conclusion

Confinement and curvature modulate the forces between nanomaterials and their environment, and hold the key to its final properties. The responsive behavior of engineered nanomaterials follows from a non-trivial interplay between NP size, shape, and surface functionalization. Although a great deal of work has been directed towards characterizing the effect of NP size and shape on its circulation time and cellular internalization, the role they play in the responsiveness of the final nanoconstruct remains unclear. In functionalized nanomaterials, the organization and chemical state of the soft and biological ligands confined onto its surface depend on the interplay between physical and chemical interactions. Our selection of the literature highlights this competition and the way it is modulated by the geometry of the nano-bio interface in very relevant biomedical scenarios. The unambiguous relation between structure and activity breaks down, and the properties of the end-tethered ligands become dependent on the confining surface curvature and on the local molecular environment. Acknowledging the coupling between molecular organization, chemical equilibria and physical interactions is key to understand the chemical and biological activity of responsive bionanomaterials, and to then translate this understanding into rational guidelines for their design.

The creativity and efforts in NP-based drug research have not had a very successful clinical translation so far, as only a couple of drugs resulting from these formulations had reached the market.¹²⁷ The difficulty for this technological transfer follows from the uncertainties on the fate of nanomaterials *in vivo*, their toxicity and that of their by-products.⁷³ Characterizing engineered NPs' intrinsic physicochemical properties is not enough.

Tailoring their interactions with physiological systems is mandatory to control their biocompatibility, biodistribution and site-specific recognition. Pragmatic approaches resort to empirical screening and combinatorial analysis of hundreds or thousands of different NP constructs to find candidates with optimized *in vivo* performance (see Figure 4) in order to profile nanomaterials biological activities. Even though correlations can be drawn from such approaches, their origins remain unknown, limiting their reach of applicability.¹²⁸

Understanding the fundamentals at the nano-bio interface is what makes the difference and will lead to ability to molecularly design nanomaterials for *in vivo* applications. Interdisciplinary approaches that combine nanotechnology, soft materials, molecular biology and medicine are required. Resorting not only to state of the art experimental techniques for the *in vitro* and *in vivo* characterization of bionanomaterials, but also to theory and molecular modeling methods. The growing interplay between theory and experiments stresses the strength of an adequate molecular modeling to gain further fundamental understanding. Multiscale computational approaches would also impart more versatility, as they have the flexibility to explore parameters out of reach for experiments. Moreover, validated theoretical and computational methods hold great promise as predictive and profiling tools, first optimizing various physicochemical properties *in silico*, then guiding and narrowing the scope of *in vitro* and *in vivo* experiments. Exploiting the complementarity of experimental and computational methodologies has the potential to complete the description of complex biochemical life processes and to predict the fate of tailored nanomaterials in biological systems. This interdisciplinary strategy, as applied in the last few years, enabled the understanding of the important parameters that determine the behavior of these responsive systems as described in this review. Therefore, we believe that its extension to more complex systems is the path for closing the gap between the lab bench and the patient.

Acknowledgments

This research was supported by Grant No. EB005772 from the National Institute of Biomedical Imaging and Bioengineering (NIBIB) at the National Institutes of Health (NIH) and by grant CBET-1403058 from the National Science Foundation (NSF).

References

1. Ariga, K. RSC Nanoscience & Nanotechnology. Royal Society of Chemistry; 2012. Manipulation of Nanoscale Materials : An Introduction to Nanoarchitectonics.
2. Maruccio G, Cingolani R, Rinaldi R. Projecting the nanoworld: Concepts, results and perspectives of molecular electronics. Journal of Materials Chemistry. 2004; 14:542.10.1039/b311929g
3. Huang J, Momenzadeh M, Lombardi F. An overview of nanoscale devices and circuits. Design & Test of Computers, IEEE. 2007; 24:304–311.10.1109/MDT.2007.121
4. Linares N, Silvestre-Albero AM, Serrano E, Silvestre-Albero J, García-Martínez J. Mesoporous materials for clean energy technologies. Chem Soc Rev. 2014; 43:7681–7717.10.1039/C3CS60435G [PubMed: 24699503]
5. Chen G, Seo J, Yang C, Prasad PN. Nanochemistry and nanomaterials for photovoltaics. Chem Soc Rev. 2013; 42:8304.10.1039/c3cs60054h [PubMed: 23868557]
6. Khin MM, Nair AS, Babu VJ, Murugan R, Ramakrishna S. A review on nanomaterials for environmental remediation. Energy & Environmental Science. 2012; 5:8075–8109.10.1039/C2EE21818F

7. Petros RA, DeSimone JM. Strategies in the design of nanoparticles for therapeutic applications. 2010;1–13.10.1038/nrd2591.
8. Kujawa P, Winnik FM. Innovation in Nanomedicine through Materials Nanoarchitectonics. *Langmuir*. 2013; 29:7354–7361.10.1021/la4014619 [PubMed: 23611489]
9. Ahmed N, Fessi H, Elaissari A. Theranostic applications of nanoparticles in cancer. *Drug Discovery Today*. 2012; 17:928–934.10.1016/j.drudis.2012.03.010 [PubMed: 22484464]
10. Mura S, Nicolas J, Couvreur P. Stimuli-responsive nanocarriers for drug delivery. *Nature Materials*. 2013; 12:991–1003.10.1038/nmat3776 [PubMed: 24150417]
11. Gao W, Chan JM, Farokhzad OC. pH-Responsive Nanoparticles for Drug Delivery. *Mol Pharmaceutics*. 2010; 7:1913–1920.10.1021/mp100253e
12. Kamaly N, Xiao Z, Valencia PM, Radovic-Moreno AF, Farokhzad OC. Targeted polymeric therapeutic nanoparticles: design, development and clinical translation. *Chem Soc Rev*. 2012; 41:2971.10.1039/c2cs15344k [PubMed: 22388185]
13. Sumer B, Gao J. Theranostic nanomedicine for cancer. *Nanomedicine*. 2008; 3:137–140.10.2217/17435889.3.2.137 [PubMed: 18373419]
14. Lammers T, Kiessling F, Hennink WE, Storm G. Drug targeting to tumors: Principles, pitfalls and (pre-) clinical progress. *Journal of Controlled Release*. 2012; 161:175–187.10.1016/j.jconrel.2011.09.063 [PubMed: 21945285]
15. Tagliacruzchi M, Peleg O, Kröger M, Rabin Y, Szeifer I. Effect of charge, hydrophobicity, and sequence of nucleoporins on the translocation of model particles through the nuclear pore complex. *Proc Natl Acad Sci US A*. 2013; 110:3363–3368.10.1073/pnas.1212909110
16. Richter K, Nessling M, Lichter P. Experimental evidence for the influence of molecular crowding on nuclear architecture. *Journal of Cell Science*. 2007; 120:1673–1680.10.1242/jcs.03440 [PubMed: 17430977]
17. Nap RJ, Szeifer I. How to optimize binding of coated nanoparticles: coupling of physical interactions, molecular organization and chemical state. *Biomater Sci*. 2013; 1:814.10.1039/c3bm00181d [PubMed: 23930222]
18. Kim JS, Backman V, Szeifer I. Crowding-Induced Structural Alterations of Random-Loop Chromosome Model. *Physical Review Letters*. 2011; 106:168102.10.1103/PhysRevLett.106.168102 [PubMed: 21599416]
19. Tagliacruzchi M, Szeifer I. Stimuli-responsive polymers grafted to nanopores and other nano-curved surfaces: structure, chemical equilibrium and transport. *Soft Matter*. 2012; 8:7292.10.1039/c2sm25777g
20. Moghimi SM, Peer D, Langer R. Reshaping the Future of Nanopharmaceuticals: Ad Iudicium. *ACS Nano*. 2011; 5:8454–8458.10.1021/nn2038252 [PubMed: 21992178]
21. Rai P, Mallidi S, Zheng X, Rahmzadeh R, Mir Y, Elrington S, Khurshid A, Hasan T. Development and applications of photo-triggered theranostic agents. *Advanced Drug Delivery Reviews*. 2010; 62:1094–1124.10.1016/j.addr.2010.09.002 [PubMed: 20858520]
22. Xie J, Lee S, Chen X. Nanoparticle-based theranostic agents. *Advanced Drug Delivery Reviews*. 2010; 62:1064–1079.10.1016/j.addr.2010.07.009 [PubMed: 20691229]
23. Kim J, Piao Y, Hyeon T. Multifunctional nanostructured materials for multimodal imaging, and simultaneous imaging and therapy. *Chemical Society Reviews*. 2009; 38:372.10.1039/b709883a [PubMed: 19169455]
24. Whitesides GM. The “right” size in nanobiotechnology. *Nature Biotechnology*. 2003; 21:1161–1165.10.1038/nbt872
25. Nel AE, Mädler L, Velegol D, Xia T, Hoek EMV, Somasundaran P, Klaessig F, Castranova V, Thompson M. Understanding biophysicochemical interactions at the nano–bio interface. *Nature Materials*. 2009; 8:543–557.10.1038/nmat2442 [PubMed: 19525947]
26. Tong R, Tang L, Ma L, Tu C, Baumgartner R, Cheng J. Smart chemistry in polymeric nanomedicine. *Chem Soc Rev*. 2014.10.1039/c4cs00133h
27. Cho K, Wang X, Nie S, Chen Z, Shin DM. Therapeutic Nanoparticles for Drug Delivery in Cancer. *Clinical Cancer Research*. 2008; 14:1310–1316.10.1158/1078-0432.CCR-07-1441 [PubMed: 18316549]

28. Lacerda L, Bianco A, Prato M, Kostarelos K. Carbon nanotubes as nanomedicines: From toxicology to pharmacology. *Advanced Drug Delivery Reviews*. 2006; 58:1460–1470.10.1016/j.addr.2006.09.015 [PubMed: 17113677]
29. Sharifi S, Behzadi S, Laurent S, Laird Forrest M, Stroeve P, Mahmoudi M. Toxicity of nanomaterials. *Chem Soc Rev*. 2012; 41:2323.10.1039/c1cs15188f [PubMed: 22170510]
30. Dobrovolskaia MA, McNeil SE. Immunological properties of engineered nanomaterials. *Nature Nanotechnology*. 2007; 2:469–478.10.1038/nnano.2007.223
31. Mout R, Moyano DF, Rana S, Rotello VM. Surface functionalization of nanoparticles for nanomedicine. *Chem Soc Rev*. 2012; 41:2539.10.1039/c2cs15294k [PubMed: 22310807]
32. Jain RK, Stylianopoulos T. Delivering nanomedicine to solid tumors. *Nature Publishing Group*. 2010; 7:653–664.10.1038/nrclinonc.2010.139
33. Ho Y-P, Leong KW. Quantum dot-based theranostics. *Nanoscale*. 2010; 2:60.10.1039/b9nr00178f [PubMed: 20648364]
34. Xie J, Huang J, Li X, Sun S, Chen X. Iron oxide nanoparticle platform for biomedical applications. *Current Medicinal Chemistry*. 2009; 16:1278–1294.10.2174/092986709787846604 [PubMed: 19355885]
35. Dreaden EC, Alkilany AM, Huang X, Murphy CJ, El-Sayed MA. The golden age: gold nanoparticles for biomedicine. *Chem Soc Rev*. 2012; 41:2740.10.1039/c1cs15237h [PubMed: 22109657]
36. Idris NM, Gnanasammandhan MK, Zhang J, Ho PC, Mahendran R, Zhang Y. In vivo photodynamic therapy using upconversion nanoparticles as remote-controlled nanotransducers. *Nature Medicine*. 2012; 18:1580–1585.10.1038/nm.2933
37. Li Z, Barnes JC, Bosoy A, Stoddart JF, Zink JI. Mesoporous silica nanoparticles in biomedical applications. *Chemical Society Reviews*. 2012; 41:2590.10.1039/c1cs15246g [PubMed: 22216418]
38. Xiong X-B, Falamarzian A, Garg SM, Lavasanifar A. Engineering of amphiphilic block copolymers for polymeric micellar drug and gene delivery. *Journal of Controlled Release*. 2011; 155:248–261.10.1016/j.jconrel.2011.04.028 [PubMed: 21621570]
39. Mintzer MA, Grinstaff MW. Biomedical applications of dendrimers: a tutorial. *Chemical Society Reviews*. 2010; 40:173.10.1039/b901839p [PubMed: 20877875]
40. Chacko RT, Ventura J, Zhuang J, Thayumanavan S. Polymer nanogels: A versatile nanoscopic drug delivery platform. *Advanced Drug Delivery Reviews*. 2012; 64:836–851.10.1016/j.addr.2012.02.002 [PubMed: 22342438]
41. Immordino ML, Dosio F, Cattel L. Stealth liposomes: review of the basic science, rationale, and clinical applications, existing and potential. *International journal of nanomedicine*. 2006; 1:297–315. [PubMed: 17717971]
42. Yildiz I, Shukla S, Steinmetz NF. Applications of viral nanoparticles in medicine. *Current Opinion in Biotechnology*. 2011; 22:901–908.10.1016/j.copbio.2011.04.020 [PubMed: 21592772]
43. Langille MR, Personick ML, Zhang J, Mirkin CA. Defining Rules for the Shape Evolution of Gold Nanoparticles. *Journal of the American Chemical Society*. 2012; 134:14542–14554.10.1021/ja305245g [PubMed: 22920241]
44. Grzelczak M, Pérez-Juste J, Mulvaney P, Liz-Marzán LM. Shape control in gold nanoparticle synthesis. *Chemical Society Reviews*. 2008; 37:1783.10.1039/b711490g [PubMed: 18762828]
45. Guerrero-Martínez A, Barbosa S, Pastoriza-Santos I, Liz-Marzán LM. Nanostars shine bright for you. *Current Opinion in Colloid & Interface Science*. 2011; 16:118–127.10.1016/j.cocis.2010.12.007
46. Dam DHM, Lee JH, Sisco PN, Co DT, Zhang M, Wasielewski MR, Odom TW. Direct Observation of Nanoparticle–Cancer Cell Nucleus Interactions. *ACS Nano*. 2012; 6:3318–3326.10.1021/nn300296p [PubMed: 22424173]
47. Black KCL, Wang Y, Luehmann HP, Cai X, Xing W, Pang B, Zhao Y, Cutler CS, Wang LV, Liu Y, et al. Radioactive ¹⁹⁸Au-Doped Nanostructures with Different Shapes for In Vivo Analyses of Their Biodistribution, Tumor Uptake, and Intratumoral Distribution. *ACS Nano*. 2014; 8:4385–4394.10.1021/nn406258m [PubMed: 24766522]

48. Matsumura Y, Maeda H. A new concept for macromolecular therapeutics in cancer chemotherapy: Mechanism of tumoritropic accumulation of proteins and the antitumor agent smancs. *Cancer Research*. 1986; 46:6387–6392. [PubMed: 2946403]
49. Torchilin V. Tumor delivery of macromolecular drugs based on the EPR effect. *Advanced Drug Delivery Reviews*. 2011; 63:131–135.10.1016/j.addr.2010.03.011 [PubMed: 20304019]
50. Alexander-Bryant AA, Berg-Foels WSV, Wen X. Bioengineering Strategies for Designing Targeted Cancer Therapies. *Advances in Cancer Research*. 2013; 118:1–59.10.1016/B978-0-12-407173-5.00002-9 [PubMed: 23768509]
51. Chou LYT, Ming K, Chan WCW. Strategies for the intracellular delivery of nanoparticles. *Chemical Society Reviews*. 2010; 40:233.10.1039/c0cs00003e [PubMed: 20886124]
52. Bertrand N, Wu J, Xu X, Kamaly N, Farokhzad OC. Cancer nanotechnology: The impact of passive and active targeting in the era of modern cancer biology. *Advanced Drug Delivery Reviews*. 2014; 66:2–25.10.1016/j.addr.2013.11.009 [PubMed: 24270007]
53. Sapsford KE, Algar WR, Berti L, Gemmill KB, Casey BJ, Oh E, Stewart MH, Medintz IL. Functionalizing Nanoparticles with Biological Molecules: Developing Chemistries that Facilitate Nanotechnology. *Chemical Reviews*. 2013; 113:1904–2074.10.1021/cr300143v [PubMed: 23432378]
54. Gil ES, Hudson SM. Stimuli-responsive polymers and their bioconjugates. *Progress in Polymer Science*. 2004; 29:1173–1222.10.1016/j.progpolymsci.2004.08.003
55. Huo M, Yuan J, Tao L, Wei Y. Redox-responsive polymers for drug delivery: from molecular design to applications. *Polymer Chemistry*. 2014; 5:1519–1528.10.1039/C3PY01192E
56. de la Rica R, Aili D, Stevens MM. Enzyme-responsive nanoparticles for drug release and diagnostics. *Advanced Drug Delivery Reviews*. 2012; 64:967–978.10.1016/j.addr.2012.01.002 [PubMed: 22266127]
57. Klouda L, Mikos AG. Thermoresponsive hydrogels in biomedical applications. *European Journal of Pharmaceutics and Biopharmaceutics*. 2008; 68:34–45.10.1016/j.ejpb.2007.02.025 [PubMed: 17881200]
58. Roy D, Brooks WLA, Sumerlin BS. New directions in thermoresponsive polymers. *Chemical Society Reviews*. 2013; 42:7214–7243.10.1039/C3CS35499G [PubMed: 23450220]
59. Medeiros SF, Santos AM, Fessi H, Elaissari A. Stimuli-responsive magnetic particles for biomedical applications. *International Journal of Pharmaceutics*. 2011; 403:139–161.10.1016/j.ijpharm.2010.10.011 [PubMed: 20951779]
60. Sirsi SR, Borden MA. State-of-the-art materials for ultrasound-triggered drug delivery. *Advanced Drug Delivery Reviews*. 2014; 72:3–14.10.1016/j.addr.2013.12.010 [PubMed: 24389162]
61. Shanmugam V, Selvakumar S, Yeh C-S. Near-infrared light-responsive nanomaterials in cancer therapeutics. *Chem Soc Rev*. 2014; 43:6254–6287.10.1039/C4CS00011K [PubMed: 24811160]
62. Stuart MAC, Huck WTS, Genzer J, Müller M, Ober C, Stamm M, Sukhorukov GB, Szeifer I, Tsukruk VV, Urban M, et al. Emerging applications of stimuli-responsive polymer materials. *Nature Materials*. 2010; 9:101–113.10.1038/nmat2614 [PubMed: 20094081]
63. Tagliazucchi M, Szeifer I. Transport mechanisms in nanopores and nanochannels: can we mimic nature? *Biochemical Pharmacology*. 2015; 18:131–142.10.1016/j.mattod.2014.10.020
64. Nap R, Gong P, Szeifer I. Weak polyelectrolytes tethered to surfaces: Effect of geometry, acid–base equilibrium and electrical permittivity. *J Polym Sci B Polym Phys*. 2006; 44:2638–2662.10.1002/polb.20896
65. Wang D, Nap RJ, Lagzi In, Kowalczyk B, Han S, Grzybowski BA, Szeifer I. How and Why Nanoparticle’s Curvature Regulates the Apparent pKa of the Coating Ligands. *J Am Chem Soc*. 2011; 133:2192–2197.10.1021/ja108154a [PubMed: 21280574]
66. Vayssieres L. On the Effect of Nanoparticle Size on Water-Oxide Interfacial Chemistry. *The Journal of Physical Chemistry C*. 2009; 113:4733–4736.10.1021/jp810721f
67. Brown MA, Duyckaerts N, Redondo AB, Jordan I, Nolting F, Kleibert A, Ammann M, Wörner HJ, van Bokhoven JA, Abbas Z. Effect of Surface Charge Density on the Affinity of Oxide Nanoparticles for the Vapor–Water Interface. *Langmuir*. 2013; 29:5023–5029.10.1021/la4005054 [PubMed: 23534618]

68. Nap RJ, Park Y, Wong JY, Szeifer I. Adsorption of Acid and Polymer Coated Nanoparticles: A Statistical Thermodynamics Approach. *Langmuir*. 2013; 29:14482–14493.10.1021/la403143a [PubMed: 24143965]
69. Ma Y, Nolte RJM, Cornelissen JJLM. Virus-based nanocarriers for drug delivery. *Advanced Drug Delivery Reviews*. 2012; 64:811–825.10.1016/j.addr.2012.01.005 [PubMed: 22285585]
70. Busseron E, Ruff Y, Moulin E, Giuseppone N. Supramolecular self-assemblies as functional nanomaterials. *Nanoscale*. 2013; 5:7098–7140.10.1039/c3nr02176a [PubMed: 23832165]
71. Nap RJ, Boži AL, Szeifer I, Podgornik R. The Role of Solution Conditions in the Bacteriophage PP7 Capsid Charge Regulation. *Biophysj*. 2014;1–10.10.1016/j.bpj.2014.08.032.
72. Monopoli MP, Åberg C, Salvati A, Dawson KA. Biomolecular coronas provide the biological identity of nanosized materials. *Nature Nanotechnology*. 2012; 7:779–786.10.1038/nnano.2012.207
73. Walkey CD, Chan WCW. Understanding and controlling the interaction of nanomaterials with proteins in a physiological environment. *Chemical Society Reviews*. 2012; 41:2780.10.1039/c1cs15233e [PubMed: 22086677]
74. Khlebtsov N, Dykman L. Biodistribution and toxicity of engineered gold nanoparticles: a review of in vitro and in vivo studies. *Chemical Society Reviews*. 2011; 40:1647.10.1039/c0cs00018c [PubMed: 21082078]
75. Lundqvist M, Stigler J, Elia G, Lynch I, Cedervall T, Dawson KA. Nanoparticle size and surface properties determine the protein corona with possible implications for biological impacts. *Proceedings of the National Academy of Sciences*. 2008; 105:14265–14270.10.1073/pnas.0805135105
76. Saptarshi SR, Duschl A, Lopata AL. Interaction of nanoparticles with proteins: relation to bio-reactivity of the nanoparticle. *Journal of Nanobiotechnology*. 2013; 11:1–1.10.1186/1477-3155-11-26 [PubMed: 23343139]
77. Roach P, Farrar D, Perry CC. Interpretation of Protein Adsorption: Surface-Induced Conformational Changes. *J Am Chem Soc*. 2005; 127:8168–8173.10.1021/ja042898o [PubMed: 15926845]
78. Lundqvist M, Sethson I, Jonsson B-H. Protein Adsorption onto Silica Nanoparticles: Conformational Changes Depend on the Particles' Curvature and the Protein Stability. *Langmuir*. 2004; 20:10639–10647.10.1021/la0484725 [PubMed: 15544396]
79. Walkey CD, Olsen JB, Song F, Liu R, Guo H, Olsen DWH, Cohen Y, Emili A, Chan WCW. Protein Corona Fingerprinting Predicts the Cellular Interaction of Gold and Silver Nanoparticles. *ACS Nano*. 2014; 8:2439–2455.10.1021/nn406018q [PubMed: 24517450]
80. Lu HB, Campbell CT, Castner DG. Attachment of Functionalized Poly(ethylene glycol) Films to Gold Surfaces. *Langmuir*. 2000; 16:1711–1718.10.1021/la990221m
81. Harder P, Grunze M, Dahint R, Whitesides GM, Laibinis PE. Molecular conformation in oligo(ethylene glycol)-terminated self-assembled monolayers on gold and silver surfaces determines their ability to resist protein adsorption. *The Journal of Physical Chemistry B*. 1998; 102:426–436.10.1021/jp972635z
82. Huang C-J, Li Y, Jiang S. Zwitterionic Polymer-Based Platform with Two-Layer Architecture for Ultra Low Fouling and High Protein Loading. *Analytical Chemistry*. 2012; 84:3440–3445.10.1021/ac3003769 [PubMed: 22409836]
83. Osterberg E, Bergström K, Holmberg K, Schuman TP, Riggs JA, Burns NL, Van Alstine JM, Harris JM. Protein-rejecting ability of surface-bound dextran in end-on and side-on configurations: comparison to PEG. *Journal of biomedical materials research*. 1995; 29:741–747.10.1002/jbm.820290610 [PubMed: 7593011]
84. Lau KHA, Ren C, Sileika TS, Park SH, Szeifer I, Messersmith PB. Surface-Grafted Polysarcosine as a Peptoid Antifouling Polymer Brush. *Langmuir*. 2012; 28:16099–16107.10.1021/la302131n [PubMed: 23101930]
85. Lau KHA, Ren C, Park SH, Szeifer I, Messersmith PB. An Experimental-Theoretical Analysis of Protein Adsorption on Peptidomimetic Polymer Brushes. *Langmuir*. 2012; 28:2288–2298.10.1021/la203905g [PubMed: 22107438]

86. Ham HO, Park SH, Kurutz JW, Szeleifer IG, Messersmith PB. Antifouling Glycocalyx-Mimetic Peptoids. *J Am Chem Soc.* 2013; 135:13015–13022.10.1021/ja404681x [PubMed: 23919653]
87. Satulovsky J, Carignano MA, Szeleifer I. Kinetic and thermodynamic control of protein adsorption. *Proc Natl Acad Sci US A.* 2000; 97:9037–9041.10.1073/pnas.150236197
88. Fang F, Szeleifer I. Competitive adsorption in model charged protein mixtures: equilibrium isotherms and kinetics behavior. *J Chem Phys.* 2003; 119:1053–1065.10.1063/1.1578992
89. Szeleifer I. Protein adsorption on surfaces with grafted polymers: A theoretical approach. *Biophys J.* 1997; 72:595–612. [PubMed: 9017189]
90. Walkey CD, Olsen JB, Guo H, Emili A, Chan WCW. Nanoparticle Size and Surface Chemistry Determine Serum Protein Adsorption and Macrophage Uptake. *J Am Chem Soc.* 2012; 134:2139–2147.10.1021/ja2084338 [PubMed: 22191645]
91. Carignano MA, Szeleifer I. Structural and thermodynamic properties of end-grafted polymers on curved surfaces. *J Chem Phys.* 1995; 102:8662–8669.10.1063/1.468968
92. Gagner JE, Lopez MD, Dordick JS, Siegel RW. Effect of gold nanoparticle morphology on adsorbed protein structure and function. *Biomaterials.* 2011; 32:7241–7252.10.1016/j.biomaterials.2011.05.091 [PubMed: 21705074]
93. Treuel L, Eslahian KA, Docter D, Lang T, Zellner R, Nienhaus K, Nienhaus GU, Stauber RH, Maskos M. Physicochemical characterization of nanoparticles and their behavior in the biological environment. *Phys Chem Chem Phys.* 2014; 16:15053.10.1039/c4cp00058g [PubMed: 24943742]
94. Halperin A. Polymer Brushes that Resist Adsorption of Model Proteins: Design Parameters. *Langmuir.* 1999; 15:2525–2533.10.1021/la981356f
95. McPherson T, Kidane A, Szeleifer I, Park K. Prevention of protein adsorption by tethered poly (ethylene oxide) layers: experiments and single-chain mean-field analysis. *Langmuir.* 1998.10.1021/la9706781.
96. Statz AR, Kuang J, Ren C, Barron AE, Szeleifer I, Messersmith PB. Experimental and theoretical investigation of chain length and surface coverage on fouling of surface grafted polypeptoids. *Biointerphases.* 2009; 4:FA22.10.1116/1.3115103. [PubMed: 20300542]
97. Szeleifer I, Carignano MA. Tethered polymer layers: phase transitions and reduction of protein adsorption. *Macromolecular Rapid Communications.* 2000; 21:423–448.
98. Canton I, Battaglia G. Endocytosis at the nanoscale. *Chemical Society Reviews.* 2012; 41:2718.10.1039/c2cs15309b [PubMed: 22389111]
99. Shang L, Nienhaus K, Nienhaus GU. Engineered nanoparticles interacting with cells: size matters. *Journal of Nanobiotechnology.* 2014; 12:1–11.10.1186/1477-3155-12-5 [PubMed: 24411017]
100. Verma A, Stellacci F. Effect of Surface Properties on Nanoparticle–Cell Interactions. *Small.* 2010; 6:12–21.10.1002/sml.200901158 [PubMed: 19844908]
101. Gratton SEA, Ropp PA, Pohlhaus PD, Luft JC, Madden VJ, Napier ME, DeSimone JM. The effect of particle design on cellular internalization pathways. *Proceedings of the National Academy of Sciences.* 2008; 105:11613–11618.10.1073/pnas.0801763105
102. Montis C, Maiolo D, Alessandri I, Bergese P, Berti D. Interaction of nanoparticles with lipid membranes: a multiscale perspective. *Nanoscale.* 2014; 6:6452.10.1039/c4nr00838c [PubMed: 24807475]
103. Chithrani BD, Ghazani AA, Chan WCW. Determining the Size and Shape Dependence of Gold Nanoparticle Uptake into Mammalian Cells. *Nano Letters.* 2006; 6:662–668.10.1021/nl052396o [PubMed: 16608261]
104. Tonga GY, Saha K, Rotello VM. 25th Anniversary Article: Interfacing Nanoparticles and Biology: New Strategies for Biomedicine. *Advanced Materials.* 2013; 26:359–370.10.1002/adma.201303001 [PubMed: 24105763]
105. Verma A, Uzun O, Hu Y, Han H-S, Watson N, Chen S, Irvine DJ, Stellacci F. Surface-structure-regulated cell-membrane penetration by monolayer-protected nanoparticles. *Nature Materials.* 2008; 7:588–595.10.1038/nmat2202 [PubMed: 18500347]
106. Cesbron Y, Shaw CP, Birchall JP, Free P, Lévy R. Stripy Nanoparticles Revisited. *Small.* 2012; 8:3714–3719.10.1002/sml.201001465 [PubMed: 23180635]
107. Nap RJ, Won Y-Y, Szeleifer I. Confinement induced lateral segregation of polymer coated nanospheres. *Soft Matter.* 2012; 8:1688.10.1039/c2sm06549e

108. Mammen M, Choi SK, Whitesides GM. Polyvalent interactions in biological systems: Implications for design and use of multivalent ligands and inhibitors. *Angew Chem Int Ed*. 1998; 37:2755–2794.
109. Gary-Bobo M, Vaillant O, Maynadier M, Basile I, Gallud A, El Cheikh K, Bouffard E, Morère A, Rébillard X, Puche P, et al. Targeting multiplicity: The key factor for anti-cancer nanoparticles. *Current Medicinal Chemistry*. 2013; 20:1946–1955.10.2174/0929867311320150002 [PubMed: 23409718]
110. Martinez-Veracochea FJ, Frenkel D. Designing super selectivity in multivalent nano-particle binding. *Proceedings of the National Academy of Sciences*. 2011; 108:10963–10968.10.1073/pnas.1105351108
111. Van Lehn RC, Alexander-Katz A. Penetration of lipid bilayers by nanoparticles with environmentally-responsive surfaces: simulations and theory. *Soft Matter*. 2011; 7:11392.10.1039/c3sm52329b
112. Van Lehn RC, Alexander-Katz A. Free energy change for insertion of charged, monolayer-protected nanoparticles into lipid bilayers. *Soft Matter*. 2013; 10:648.10.1039/c3sm52329b [PubMed: 24795979]
113. Lin J, Alexander-Katz A. Cell Membranes Open “Doors” for Cationic Nanoparticles/ Biomolecules: Insights into Uptake Kinetics. *ACS Nano*. 2013; 7:10799–10808.10.1021/nn4040553 [PubMed: 24251827]
114. Van Lehn RC, Atukorale PU, Carney RP, Yang Y-S, Stellacci F, Irvine DJ, Alexander-Katz A. Effect of Particle Diameter and Surface Composition on the Spontaneous Fusion of Monolayer-Protected Gold Nanoparticles with Lipid Bilayers. *Nano Letters*. 2013; 13:4060–4067.10.1021/nl401365n [PubMed: 23915118]
115. Van Lehn RC, Alexander-Katz A. Fusion of Ligand-Coated Nanoparticles with Lipid Bilayers: Effect of Ligand Flexibility. *J Phys Chem A*. 2014:140507111529003.10.1021/jp411662c
116. Yang K, Ma Y-q. Computer simulation of the translocation of nanoparticles with different shapes across a lipid bilayer. *Nature Nanotechnology*. 2010; 5:579–583.10.1038/nnano.2010.141
117. Howes DP, Rana S, Stevens MM. Plasmonic nanomaterials for biodiagnostics. *Chem Soc Rev*. 2014; 43:3835.10.1039/c3cs60346f [PubMed: 24323079]
118. Xu C, Sun S. New forms of superparamagnetic nanoparticles for biomedical applications. *Advanced Drug Delivery Reviews*. 2013; 65:732–743.10.1016/j.addr.2012.10.008 [PubMed: 23123295]
119. Li K, Liu B. Polymer-encapsulated organic nanoparticles for fluorescence and photoacoustic imaging. *Chem Soc Rev*. 2014.10.1039/c4cs00014e
120. Nie L, Chen X. Structural and functional photoacoustic molecular tomography aided by emerging contrast agents. *Chem Soc Rev*. 2014.10.1039/c4cs00086b
121. Howes PD, Chandrawati R, Stevens MM. Colloidal nanoparticles as advanced biological sensors. *Science*. 2014; 346:1247390–1247390.10.1126/science.1247390 [PubMed: 25278614]
122. Kelly KL, Coronado E, Zhao LL, Schatz GC. The Optical Properties of Metal Nanoparticles: The Influence of Size, Shape, and Dielectric Environment. *J Phys Chem B*. 2003; 107:668–677.10.1021/jp026731y
123. Link S, El-Sayed MA. Shape and size dependence of radiative, non-radiative and photothermal properties of gold nanocrystals. *International Reviews in Physical Chemistry*. 2000; 19:409–453.10.1080/01442350050034180
124. Weissleder R. A clearer vision for in vivo imaging. *Nature Biotechnology*. 2001; 19:316–317.10.1038/86684
125. Peng S, McMahon JM, Schatz GC, Gray SK, Sun Y. Reversing the size-dependence of surface plasmon resonances. *Proceedings of the National Academy of Sciences*. 2010; 107:14530–14534.10.1073/pnas.1007524107
126. Tagliacucchi M, Blaber MG, Schatz GC, Weiss EA, Szeifer I. Optical Properties of Responsive Hybrid Au@Polymer Nanoparticles. *ACS Nano*. 2012; 6:8397–8406.10.1021/nn303221y [PubMed: 22954258]
127. Dawidczyk CM, Kim C, Park JH, Russell LM, Lee KH, Pomper MG, Searson PC. State-of-the-art in design rules for drug delivery platforms: Lessons learned from FDA-approved nanomedicines.

Journal of Controlled Release. 2014; 187:133–144.10.1016/j.jconrel.2014.05.036 [PubMed: 24874289]

128. Time to deliver. Vol. 32. Nature Publishing Group; 2014. p. 961-961.Editorial

Author Manuscript

Author Manuscript

Author Manuscript

Author Manuscript

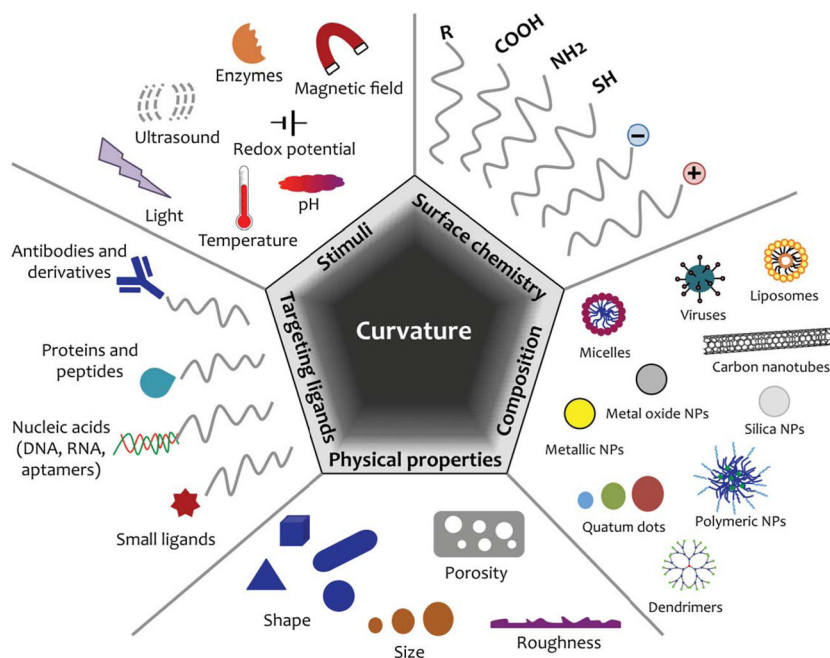


Figure 1. Design parameters for optimized smart nanomaterials for biomedical applications. Adapted in part from Kamaly *et al.*, *Chem. Soc. Rev.*, 2012, 41, 2971–3010 and from Chou *et al.*, *Chem. Soc. Rev.*, 2010, 40, 233–246 with permission of The Royal Society of Chemistry.^{12, 51}

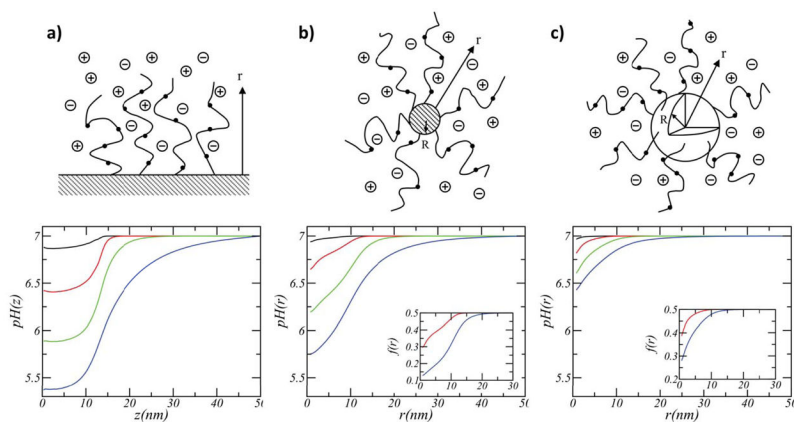


Figure 2. Variation of pH as a function of the distance from the surface for (a) planar, (b) cylindrical (1 nm diameter), and (c) spherical (1 nm diameter) NP grafted with weak polyelectrolytes (surface coverage= 0.25 nm^2 , polymer chain length= 50, and $\text{pK}_a=7$). The colors correspond to different salt concentrations: 1 (black), 0.1 (red), 0.01 (green), and 0.001 M (blue). A concentration of 0.1M is the closest to physiological conditions. The insets show the fraction of charged groups as a function of the distance from the surface. The solution's bulk pH is 7. Adapted with permission from Nap *et al.*, *J. Polym. Sci. B Polym. Phys.*, 2006, 44, 2638–2662. Copyright 2006 John Wiley & Sons, Inc. ⁶⁴

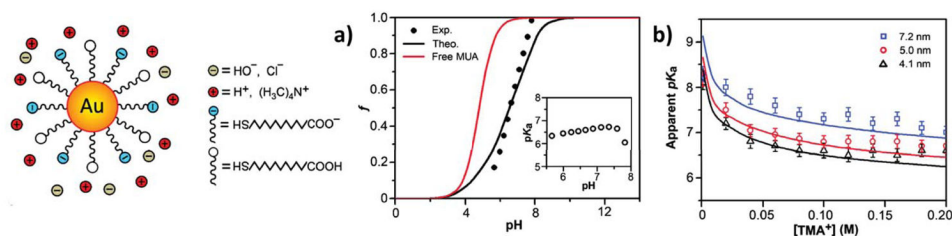


Figure 3.

(a) Fractions of dissociated MUA ligands as a function of pH. The theoretical charge fraction (black curve), f , was calculated with the molecular theory (MT). The red curve is calculated for free MUA in solution using the Henderson Hasselbalch equation. The inset shows the experimental $\text{p}K_a$ of NP's ligands. Diameter of the NP's metal core = 4.1 nm, salt concentration (tetramethylammonium chloride, TMACl) = 0.08 M. (b) The apparent $\text{p}K_a$'s of Au-MUA NPs of different sizes plotted as a function of TMACl concentration. Open markers correspond to experimental data; lines were calculated with MT. $\text{p}K_a$ for free MUA is ~ 4.8 . Adapted with permission from Wang *et al.*, *J. Am. Chem. Soc.*, 2011, 133, 2192–2197. Copyright 2011 American Chemical Society.⁶⁵

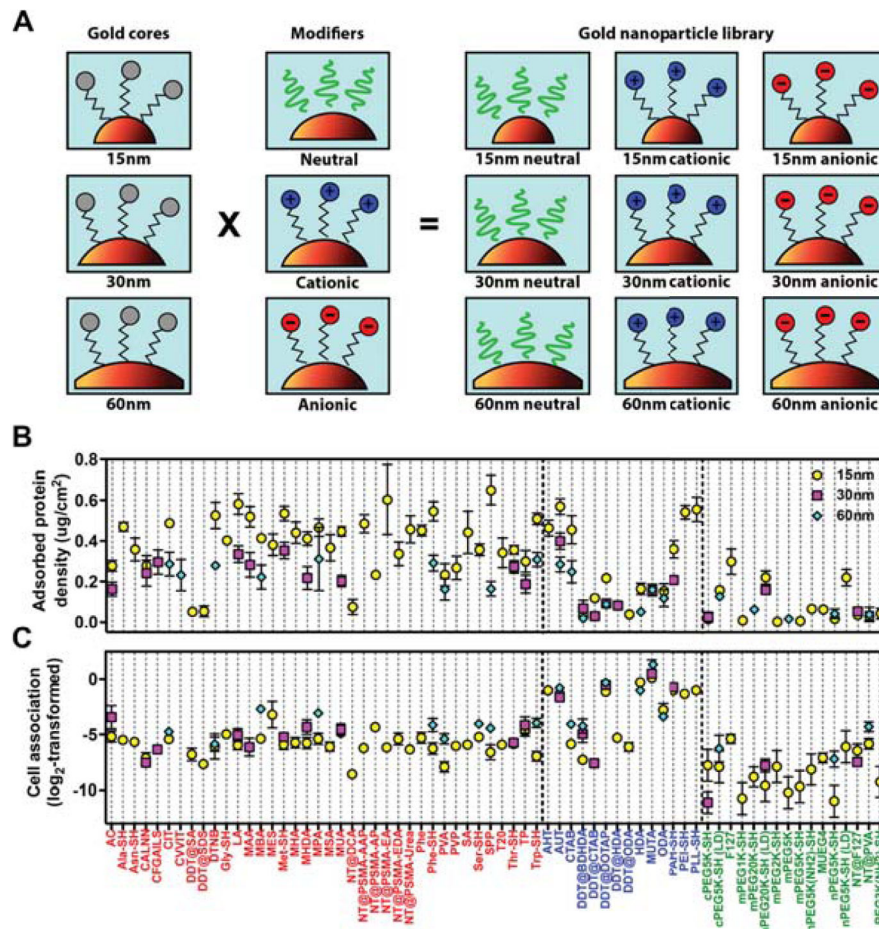


Figure 4. (A) Scheme of the combinatorial design of the Au-NP library. 105 surface-modified NP were prepared by grafting Au-NPs of 15, 30, and 60 nm diameter with 67 surface ligands of different nature: neutral (green), cationic (blue), or anionic (red). (B) Total adsorbed serum protein density, and (C) net cell association (log₂-transformed) for each formulation in the library. Adapted with permission from Walkey *et al.*, *ACS Nano*, 2014, 8, 2439–2455. Copyright 2014 American Chemical Society.⁷⁹

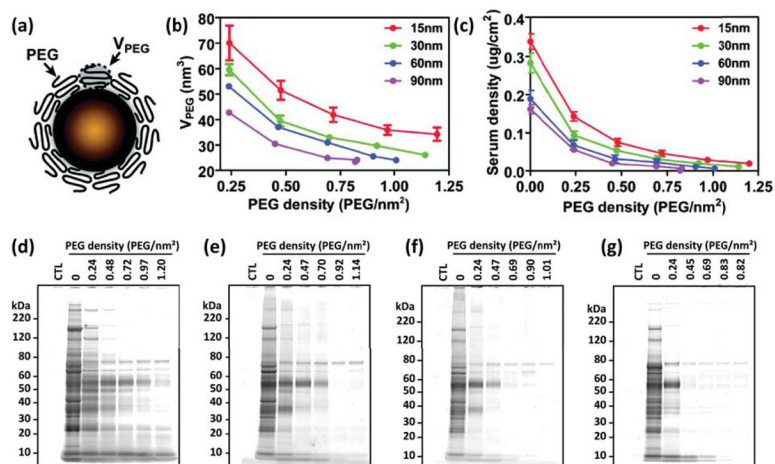


Figure 5.

(a) Scheme of a PEGylated Au-NP. (b) PEG volume as a function of the grafting density for NP of different sizes. (c) Adsorbed serum protein density as a function of PEG grafting density. (d–g) Molecular composition of the adsorbed protein layer for the 15, 30, 60 and 90 nm Au-NPs respectively. Adapted with permission from Walkey *et al.*, *J. Am. Chem. Soc.*, 2012, 134, 2139–2147. Copyright 2012 American Chemical Society.⁹⁰

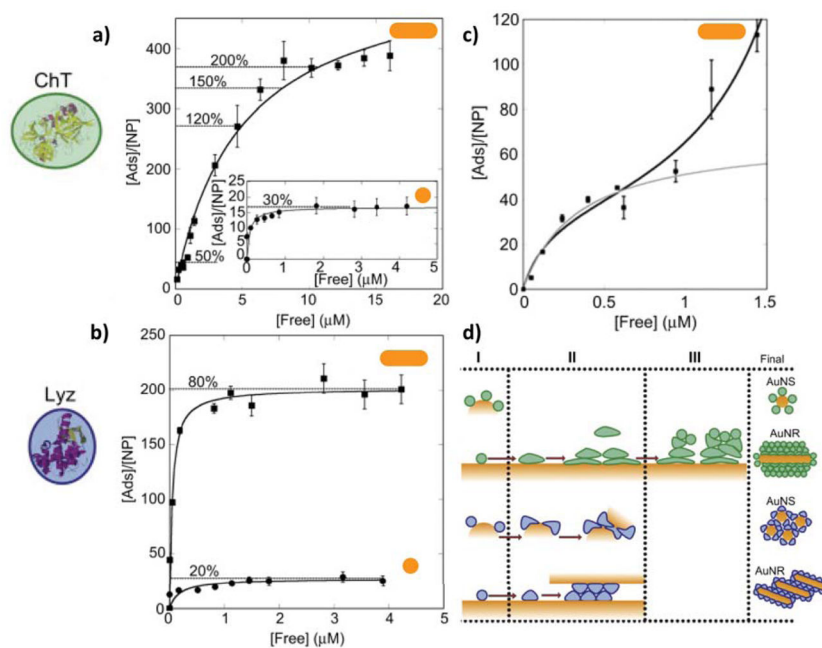


Figure 6.

a–b) Adsorption isotherms for lysozyme (Lyz) and α -chymotrypsin (ChT) onto gold nanospheres (AuNS 10.6 nm diameter) and nanorods (AuNR 10.3 nm diameter, 36.4 nm length). Solid lines correspond to the fit according to the Langmuir equation. Dotted lines indicate estimated surface coverage at the given loading. c) Adsorption isotherm for the ChT onto AuNRs, evidencing the multilayer nature of the process. d) Schematic representation of protein adsorption to AuNP. In Region I, both proteins adsorb onto the nanoparticle with almost none structural modification. In Region II, protein-surface interactions induce conformational changes. In Region III, protein-protein interactions give rise to multilayer adsorption. Reprinted and adapted from *Biomaterials*, Vol. 32, Gagner *et al.*, Effect of gold nanoparticle morphology on adsorbed protein structure and function, pp. 7241–7252, Copyright (2011), with permission from Elsevier.⁹²

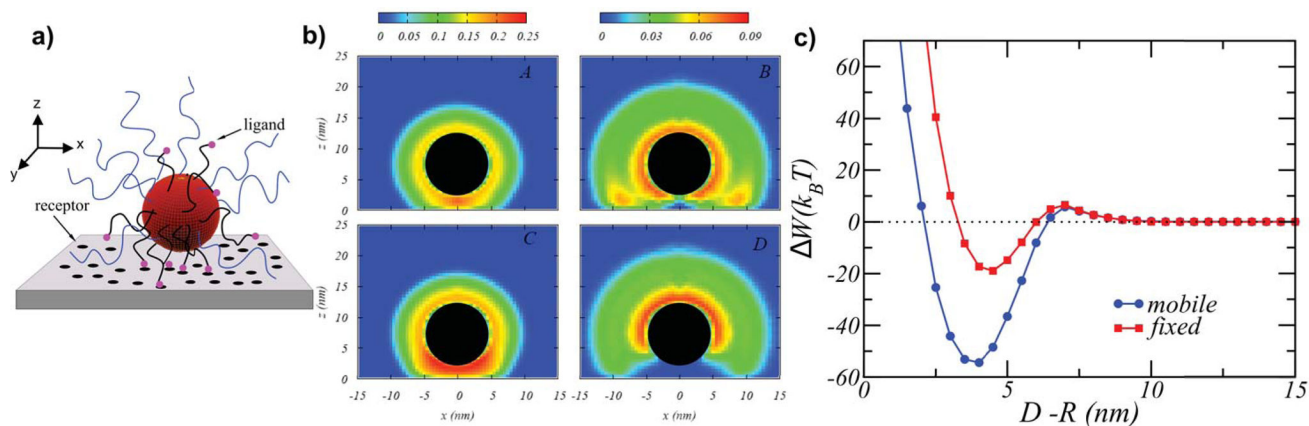


Figure 7.

a) Scheme of a polymer-coated NP interacting with a planer surface. b) Contour maps of the polymer volume fractions for the NP functionalized with short (left panel) and long (right panel) neutral polymers at a position close to the surface. Top panels (A–B) correspond to chains with no lateral mobility, while the figures in the bottom (C–D) correspond the mobile tethered chains. $R=5\text{nm}$, $\sigma=0.25$ long chains/ nm^2 , $\sigma=0.5$ short chains/ nm^2 , $N_{\text{short}}=20$ segments, $N_{\text{long}}=20$ segments. c) Free energy as a function of the distance between the NP and the surface. Adapted from Nap *et al.*, *Soft Matter*, 2012, 8, 1688–1700 with permission of The Royal Society of Chemistry.¹⁰⁷

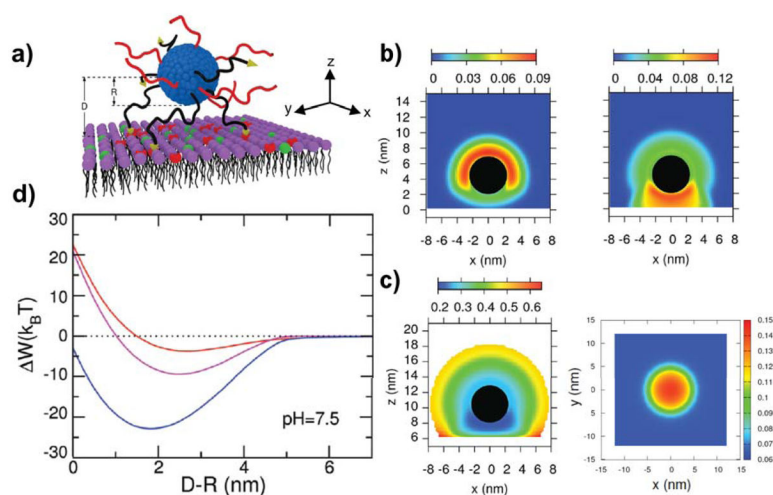
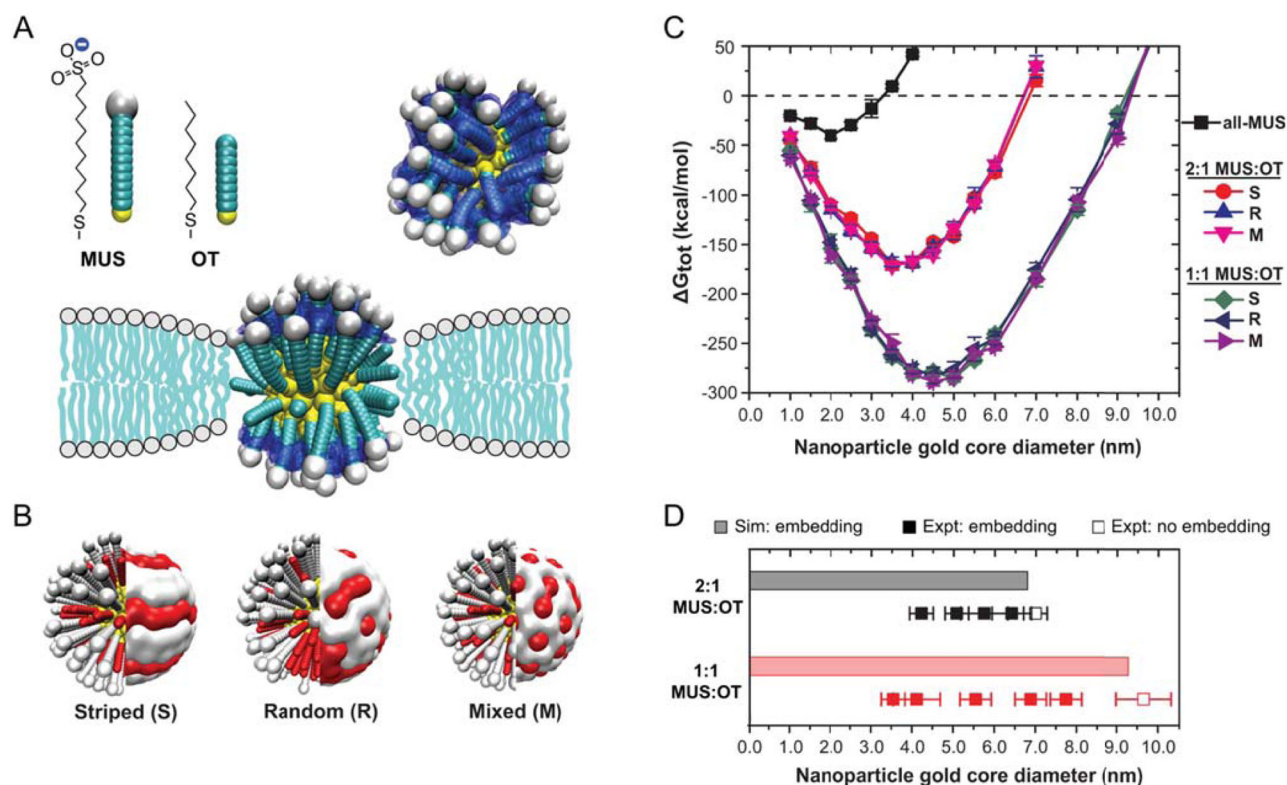


Figure 8.

a) Scheme of a polymer-coated NP interacting with a lipid membrane. Neutral polymer chains are in red, while the polybases ($pK_a=7.5$) with their ligand-end group are in black. Uncharged lipids are in purple, overexpressed receptors in red, and negatively charged lipids in green. b) Contour maps of the polymer volume fractions for both neutral polymers (left panel) and polybase (right panel) for a NP close to the lipid layer for a pH = 7.5 and a salt concentration of 0.10 M. $R=2.5\text{nm}$, $\sigma=0.20$ molecules/ nm^2 , $N=20$ segments. c) Coated NP interacting with a lipid membrane with both overexpressed receptors and charged lipids. *Left panel:* Contour map of the fraction of charged groups of the polybases on a NP close to the lipid membrane. The conditions are the same as in b). *Right panel:* Contour map of the fraction of charged lipids in the membrane. The center of the NP is at $(x; y) = (0; 0)$ and 2.0nm above the membrane surface. The conditions are the same as in b). d) Free energy as a function of the distance between the NP surface and the lipid layer. The conditions are the same as in b). The colors correspond to the three membranes modeled: no overexpressed receptors and negatively charged lipids (red), neutral lipid membrane with overexpressed receptors (magenta), and membranes with both overexpressed receptors and charged lipids (blue). Adapted and reproduced from Nap *et al.*, *Biomater. Sci.*, 2013, 1, 814–823 with permission of The Royal Society of Chemistry.¹⁷

**Figure 9.**

(A) Scheme of the simulation model based on explicit calculation of solvent-accessible surface area (blue surface). (B) Representation of the three surface morphologies simulated. (C) Simulation results for the change in free energy for embedding into the membrane as a function of AuNP core diameter. A strong dependence is observed with respect to the NP diameter and monolayer composition, but hardly non with respect to the arrangement of surface ligands. The dashed line indicates the critical size below which embedding would be favorable. (D) Comparison of simulation results from (C) to lipid membrane experiments. Reproduced with permission from Van Lehn *et al.*, *Nano Letters*, 2013, 13, 4060–4067. Copyright 2013 American Chemical Society.¹¹⁴

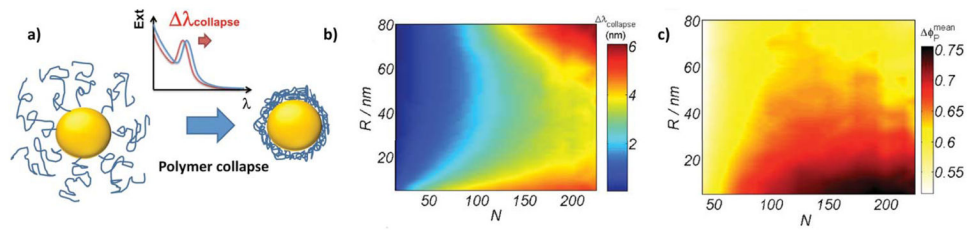


Figure 10.

a) Schematic representation of the collapse of the end-grafted polymer layer on a Au-NP due to a change in the solvent quality, and the shift in the position of the LSPR peak, $\lambda_{\text{collapse}}$, this collapse induces. b) Effect of the Au-NP core size (R) and the chain length (N) in the change in the position of the LSPR band ($\lambda_{\text{collapse}}$, panel b) and in the average polymer volume fraction of the film upon collapse ($\lambda_{\text{collapse}}$, panel c). Surface density is $\sigma = 0.5 \text{ nm}^{-2}$. Adapted with permission from Tagliazucchi *al.*, *ACS Nano*, 2012, 6, 8397–8406. Copyright 2012 American Chemical Society.¹²⁶